Title:

The study on mechanism of neuronal cell death in amyotrophic lateral sclerosis regarding U6 snRNA expression change.

（**U6 snRNA** の発現量変動に着目した筋委縮性側索硬化症における神経細胞死機構に関する研究）

北海道大学　生命科学院　生命融合科学コース

細胞機能科学研究室

矢　原　　真　郎

2018 年 3 月

Contents

Abbreviation

18S rRNA: 18S ribosomal ribonucleic acid
ALS: Amyotrophic lateral sclerosis
CLIP: Cross-linking immunoprecipitation
CTFs of TDP-43: Carboxyl-terminal fragments of TDP-43
FUS/TLS: Fused in sarcoma/ translated in liposarcoma
NC-siRNA: Non-targeting siRNA
PCR: Polymerase chain reaction
pEV: Empty vector
PI: Propidium iodide
pU6: Plasmid DNAs encoding U6 snRNA
pmCherry-H2B: Plasmid DNAs encoding to express mCherry-tagged Histone H2B
pmCherry: Plasmid DNAs encoding mCherry
pmEGFP-N1: Plasmid DNAs encoding GFP
qPCR: Real-time quantitative PCR
RNA: ribonucleic acid
RT-PCR: Reverse transcription PCR
RT-qPCR: Reverse transcription quantitative PCR
SMA: Spinal muscular atrophy
siRNA-Alexa: 555SiRNA labeled with Alexa-fluor-555
snRNAs: Small nuclear RNAs
snRNPs: Small nuclear ribonucleoproteins
SnoRNA202: Small nucleolar RNA 202
T43-GFP: C-terminally GFP-tagged TDP-43
T43-siRNA: TDP-43-targeting siRNA duplex
TDP-43-GFP: C-terminally GFP-tagged TDP-43
TDP-43: (TAR) RNA/DNA-binding protein 43 kDa
U snRNA: Uridine small nuclear RNA
U6-siRNA: U6 snRNA-targeting siRNA duplex
Urea-PAGE: Urea-polyacrylamide gel electrophoresis

Chapter 1

General introduction

1. Amyotrophic lateral sclerosis (ALS)

Cellular vital activity is maintained through many functions of RNA, where coding RNA, noncoding RNA and RNA binding protein act in various ways. Disruption of RNA homeostasis results in fatal consequences such as neurodegeneration diseases which are characterized by the death of specific types of neurons [1,2]. Especially, defects in RNA splicing are implicated in many neurodegenerative diseases including Amyotrophic lateral sclerosis (ALS) [3–5].

Amyotrophic lateral sclerosis (ALS) has developed in 2-5 per 100,000 people, which is clinically characterized by progressive degeneration of motor neurons and interneurons in the brain and spinal cord [6]. Since motor neuron is degenerated, the signal to move the muscles is not transmitted and motor function is gradually diminished with the progress of the disease. As a result, most patients died within 3 to 5 years after diagnosis [6]. At present, there is still no treatment strategy for a complete recovery, therefore, elucidation of disease mechanism and establishment for treatment strategy are strongly desired as soon as possible. Recently, genetic mutations associated with the onset of amyotrophic lateral sclerosis have been reported, and more than 20 genes have been identified now [7]. Among them, there are many genes encoding RNA binding proteins with high structural similarity, and some of which are involved in RNA splicing like fused in sarcoma/ translated in liposarcoma (FUS/TLS) and transactivation response (TAR) RNA/DNA-binding protein 43 kDa (TDP-43) [8,9]. Therefore, the disruption of RNA splicing homeostasis via RNA binding protein is expected to be a key to ALS pathogenesis.

2. Transactivation response (TAR) RNA/DNA-binding protein 43 kDa (TDP-43)

Transactivation response (TAR) RNA/DNA-binding protein 43 kDa (TDP-43) has been identified as an ALS-associated protein. TDP-43 is mainly localized in the nucleus and shuttles between the nucleus and cytoplasm to maintain several RNA-associated functions (e.g., local translation, translocation, splicing, and microRNA processing) [10]. However, in motor neurons from ALS patients, TDP-43 disappears from the nucleus and appears in cytoplasmic ubiquitinated inclusion bodies, along with carboxyl-terminal fragments (CTFs) of TDP-43 [11]. For this reason, research on the pathology has been developed from the two viewpoints; gain-of-function and loss-of-function of TDP-43.

Gain-of-function of TDP-43 hypothesis focused on point that acquiring toxicity with TDP-43 aggregation which constitutes the inclusion body of TDP-43 leads to neurodegeneration. On the other hand, loss-of-function of TDP-43 hypothesis focused on the point that the abnormal localization of TDP-43 lead to neurodegeneration through the loss of normal function of TDP-43 in the nucleus.

Both gain-of-function and loss-of-function of TDP-43 are thought to play an important role in neurodegeneration, but loss-of-function is thought to be more essential. Since TDP-43 CTFs are aggregation-prone and exert cytotoxicity in neuronal and non-neuronal cell lines [12–14], toxic gain-of-function of TDP-43 and TDP-43 CTFs may be implicated in neurodegeneration. On the other hands TDP-43 knockout in murine motor neurons causes progressive motor neuron degeneration [15], indicating that loss-of-function is a putative role for neurodegeneration as seen in ALS.

TDP-43 knockout in mice exhibits early embryonic lethality [16–18] and TDP-43 depletion in various mammalian cultured cells and embryonic stem cells increases cell death proportion [19–22]. These investigations point at an essential role of TDP-43 in cell survival. Moreover, TDP-43 depletion both in murine brain and mammalian cultured cells causes widespread alterations of the RNA-splicing state such as changes in exon inclusion [23–28]. These results imply that TDP-43 loss-of-function may cause cell death through alterations of the RNA-splicing state, however, the detailed mechanism of cell death during TDP-43 loss-of-function has not been elucidated.

In this study, we highlighted the mechanism how loss-of-function of TDP-43 causes neuronal cell death regarding RNA splicing homeostasis via U6 snRNA expression levels.

Chapter 2

Expression of U6 snRNA during TDP-43 depletion

1. Introduction

1.1 SnRNAs during loss-of-function of TDP-43

An important machinery during RNA splicing in eukaryotes is the spliceosome, composed of small nuclear RNAs (snRNAs) including U1, U2, U4, U5, and U6 snRNA, in addition to a range of small nuclear ribonucleoproteins (snRNPs) [29]. Expression level of snRNAs directly affects splicing efficiency [30,31]. Therefore, it is conceivable that expression level plays an important role in maintaining the homeostasis of RNA splicing.

Reports show that the expression profiles of such snRNAs are altered in TDP-43-knocked down cultured cells and spinal cord from ALS patients [32,33]. One study reported that the expression level of U6 snRNA was decreased in the spinal cord of ALS patients, but that of U1, U2, U4, and U5 snRNA was not [32]. Conversely, another study reported that the expression level of U6 snRNA in the spinal cord of ALS patients was not decreased, whereas that of U1, U2, U4, and U5 snRNA was increased [33]. Moreover, the amount of U6 snRNA in TDP-43-knocked down human neuroblastoma SH-SY5Y cells was not decreased in either study [32,33]. Thus, TDP-43 depletion can disturb expression of snRNAs; however, the expression profile of individual snRNAs during TDP-43 depletion remains unclear.

1.2 Quantification of RNA expression

Expression level of RNA is examined by RT-qPCR or Urea-PAGE (often additionally perform northern blotting). RT-qPCR is a method in which RNA is reverse transcribed as cDNA and the amount of its cDNA is detected by qPCR using this cDNA as PCR template. qPCR amplifies the template cDNA in a PCR efficiency-dependent manner using PCR primer, and monitors the amount of the PCR product to calculate the amount of template. Since PCR efficiency is depended on PCR primer, the result of qPCR is sensitive to PCR efficiency of each PCR primer. Therefore, estimation of PCR efficiencies of PCR primers are important in qPCR. In addition, normalization is essential for highly reliable qPCR assays because it controls the variability of extraction yield, reverse transcription efficiency and PCR efficiency to allow comparison of RNA concentrations between various samples. For this reason, the MIQE guidelines are defined to quantitatively perform RT-qPCR [34]. Moreover, in order to obtain a highly

reliable evaluation on the expression level of RNA, it is also important to investigate the amount of RNA using a method different from RT-qPCR.
Urea-PAGE is a method that does not require reverse transcription and amplification steps. The RNA of which secondary structure is denatured by urea can be separated depended on molecular weight by polyacrylamide gel, and is detected as a size dependent band by Urea-PAGE.

In this chapter, in order to accurately quantification of the expression level of U6 snRNA during TDP-43 depletion, estimation of PCR efficiency of PCR primers and examination of suitable internal standards were carried out, and the expression level of U6 snRNA was quantified using RT-qPCR. In addition, Urea-PAGE was performed to verify the result of expression level of U6 snRNA obtained by RT-qPCR.

2. Material and methods

2.1 Transfection of siRNA

Murine neuroblastoma Neuro2A cells were kindly provided by Prof. Kazuhiro Nagata at Kyoto Sangyo University. The strain of the cell was as same as that in the previous studies, and culture conditions were reported previously [35][36].

Transfection condition were determined using synthesized siRNA labeled with Alexa-fluor-555 (siRNA-Alexa 555; # 14750-100, Thermo Fisher Scientific). Neuro2A cells (0.67×10^5) were plated in a 3.5 cm cell culture dish (CORNING, Corning, NY). SiRNA was transfected using 3 µL Lipofectamine RNAiMAX transfection reagent (Thermo Fisher Scientific) and 20 pmol of each siRNA in Opti-MEM I medium (Thermo Fisher Scientific). Observation were performed using an laser scanning microscopy (LSM510-ConfoCor2; Carl Zeiss, Germany).

For knockdown of TDP-43, Neuro2A cells (5.5×10^5) were plated in a 10 cm cell culture dish (CORNING, Corning, NY). A sense and antisense TDP-43-targeting siRNA duplex (T43-siRNA; 5’-GUUAGAAAGAAGUGGAAGATT-3’ and 5’-UCUUCCACUUCUUUCUAACTT-3’, respectively; synthesized by Nippon Gene, Tokyo, Japan), or a non-targeting siRNA (NC-siRNA; #AM4611; Thermo Fisher Scientific) as a negative control, were transfected using 24 µL Lipofectamine RNAiMAX transfection reagent and 160 pmol of each siRNA in Opti-MEM I medium.

2.2 PCR for mRNAs or non-coding RNAs

At 72 h after transfection, total RNA was isolated with TRIzol (Thermo Fisher Scientific) and purified using PureLink RNA Mini Kit (Thermo Fisher Scientific) according to the manufacturer's instructions. Extracts were treated with DNase I (TaKaRa, Shiga, Japan) before performing additional assays.

To detect the mRNAs, first-strand complementary DNA synthesis was performed using a transcriptase (PrimeScript; TaKaRa) according to the manufacturer's instructions. PCR was performed using a thermal cycler (Bioer Technology, Binjiang, China). The PCR was performed in a three-step protocol under the following conditions: initial denaturing at 98°C for 30 s, followed by PCR cycles (TDP-43; 27 cycle, Actin β; 20 cycle) of denaturing at 98°C for 10 s, annealing at 60°C for 30 s, and extension at 72°C for 60 s. PCR products were separated in 1% agarose gel and detected using LAS 4000 mini (Fujifilm, Tokyo, Japan).

To detect non-coding RNAs, total RNA (750 ng) was used for synthesis of first-strand cDNA using Mir-X miRNA First Strand Synthesis Kit (TaKaRa) according to the manufacturer's instructions. Real-time quantitative PCR (qPCR) was performed using SYBR Premix Ex Taq (Tli RNase H Plus; TaKaRa), ROX Reference Dye II (TaKaRa), 0.2 μM forward primer, 0.2 μM reverse primer, and 2 μL template cDNA (corresponding to 15 ng total RNA). Amplification and detection were performed using a real-time PCR system (Mx3005P; Agilent Technologies, Santa Clara, CA). The PCR was performed in a two-step protocol under the following conditions: initial denaturing at 95°C for 30 s, followed by 35 cycles of denaturing at 95°C for 10 s, and annealing/extension at 60°C for 20 s. PCR efficiencies of each primer were determined using dilution series of amplified PCR products as PCR template. PCR primers are described in Table 1. Relative expression of U6 snRNA was calculated following the equation in the previous paper [37].

Primers for PCR		
Gene	**Forward primer**	**Reverse primer**
TDP-43	5'-TTACTGATCTGGAAGTGTGGGAACGTG-3'	5'-AAACTACTGCCAAGAAACTTTATG-3'
ACTB	5'-GTGACGTTGACATCCGTAAAGA-3'	5'-GCCGGACTCATCGTACTCC-3'
U6 snRNA	5'-CTCGCTTCGGCAGCACATATACT-3'	5'-ACGCTTCACGAATTTGCGTGTC-3'
7SL RNA	5'-GGAGTTCTGGGCTGTAGTGC-3'	5'-ATCAGCACGGGAGTTTTGAC-3'
18S rRNA	5'-GTAACCCGTTGAACCCCATT-3'	5'-CCATCCAATCGGTAGTAGCG-3'
snoRNA 202	5'-AGTACTTTTGAACCCTTTTCC-3'	†Commercial primer

Table 1: List of PCR primers.

2.3 Urea-polyacrylamide gel electrophoresis (Urea-PAGE) for RNA

Samples including total extract RNA (2.75 μg) were mixed with loading buffer consisting of 1.5× Tris-acetate EDTA (TAE), 10 M urea, 10% (w/v) sucrose, 0.05% (w/v) bromophenol blue, and 0.05% (w/v) xylene cyanol, incubated at 65°C for 15 min, and kept on ice until electrophoretic separation. Samples were separated in a 12% polyacrylamide gel containing 7% urea in 1× TAE buffer. RNAs were stained using SYBR Gold (Thermo Fisher Scientific). Fluorescent intensities were detected using LAS 4000 mini (Fujifilm) using a 460 nm excitation light and a long-pass filter (Y515; Fujifilm). Quantification was performed using ImageJ 1.47 software (National Institutes of Health, Bethesda, MD).

2.4 Cross-linking immunoprecipitation (CLIP) assay

Plasmid DNAs encoding GFP (pmEGFP-N1) and pmEGFP-N1 to express C-terminally GFP-tagged TDP-43 (TDP-43-GFP) were prepared as established previously [35]. Neuro2A cells were passaged into four 10 cm culture dishes at a ratio of 1/5 and transfected using 16.0 μL Lipofectamine 2000 transfection reagent and 4.0 μg pmEGFP-N1 or TDP-43-GFP expression plasmid (TDP-43-GFP). After incubation for 30 h, the CLIP assay was performed as previously reported [38]. Cells were fixed in phosphate-buffered saline containing 3% formaldehyde and lysed by sonication. Immunoprecipitation was performed overnight at 4°C using anti-GFP monoclonal antibody-conjugated agarose beads (MBL, Nagoya, Japan). After dissociation of cross-linked complexes at 70°C, RNA was extracted, reverse-transcribed, and U6 snRNA transcripts were quantified by qPCR as described in the “PCR for mRNAs or non-coding RNAs” sub-section.

2.5 Western blotting

Western blotting was performed using 3.5 cm culture dishes and by reducing the number of cells and amounts of siRNAs and reagents to 1/8 scale, accordingly. Recovery of cell lysates and Western blotting to detect the protein amount of TDP-43 and α-tubulin were performed as previously reported [6]. In short, cells were lysed using lysis buffer (20 mM 4-(2-HydroxyEthyl)-1- Piperazine Ethane Sulfonic acid, 10%

glycerol, 0.4M NaCl, 1.5mM MgCl2, 0.1% NP-40, 0.4mM EDTA, 1 m M DTT, 1% Protease Inhibitor Cocktail, Benzonase 0.01 U/μL). Proteins were detected using the anti-TDP43 (G400; Cell Signaling Technology, Danvers, MA) or α-tubulin antibody (DM1A; Merck KGaA, Darmstadt, Germany) as primary antibody and anti-rabbit IgG (#111-035-144, The Jackson Laboratory, Bar Harbor, ME) or anti-mouse IgG (#ab97046; Abcam, Cambridge, England).

2.6 Statistics

Student's *t* test was performed to evaluate statistical significance.

3. Results

3.1. Establishment of efficient transfection condition

We first sought to evaluate the proper condition for siRNA transfection. SiRNA modified with Alexa 555 (siRNA-Alexa 555) were transfected into the various number of Neuro2A cells, and transfection efficiency was estimated by detecting the Alexa positive cells at 24 hours after transfection started.

The transfection efficiencies at 0.33×10^5 and 0.66×10^5 revealed similar value (94.9% and 94.8% to each; Fig 1), while transfection efficiencies from 0.66×10^5 to 2.00×10^5 showed tendency to reduce the averaged transfection efficiency accompany with increase of the cell number. Thus, 0.66×10^5 is the ideal cell number to make high transfection efficiency.

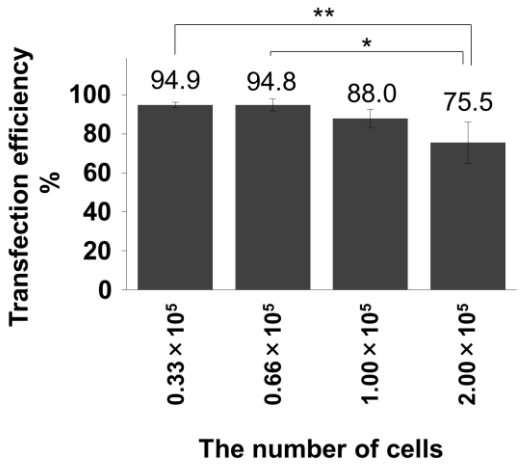

Figure 1: The dependency of transfection efficiency on the number of cells. The number of cells per 3.5 cm dish when transfection started are showed in x-axis (0.33×10^5, 0.66×10^5, 1.00×10^5 and 2.00×10^5 to each). Significance was tested by Student's *t* test*:* $*p < 0.05$ (mean ± SEM; n = 3).

3.2. Verification of TDP-43 downregulation using siRNA

Next, to knock down TDP-43, siRNA targeting TDP-43 mRNA (T43-siRNA) or non-coding siRNA (NC-siRNA) were transiently transfected into Neuro2A cells and evaluated mRNA expression using RT-PCR at 72 h after transfection. T43-siRNA-transfected cells showed approximately 70% decrease in TDP-43 levels compared with no siRNA and transfection reagents (Mock) or NC-siRNA-transfected cells. In turn, NC-siRNA transfection did not have any significant effect on the levels of TDP-43 compared with mock-transfected cells (Fig 2 A and B).

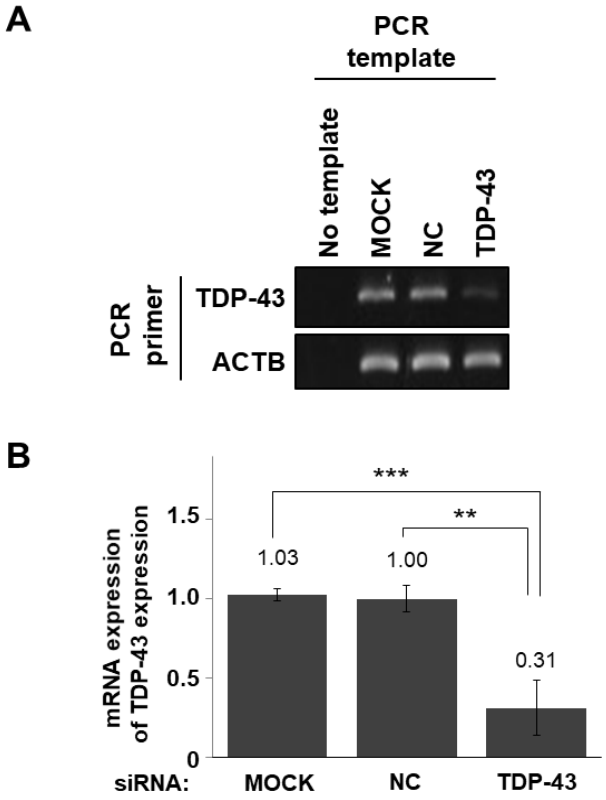

Figure 2 TDP-43 mRNA expression during TDP-43 knockdown. (A) RT-PCR results of TDP-43 expression at 72 h after transfection of T43-siRNA (TDP-43), NC-siRNA (NC), no siRNA and transfection reagents (Mock) or PCR products without addition of cDNA solution (No template). (B) Quantification of TDP-43 expression at 72 h after transfection of T43-siRNA, NC-siRNA or MOCK. The expression level of Actin-β was used as an internal control (mean ± SEM, n = 3). Significance indicated in the graph was tested by Student's *t* test: $^{**}p < 0.01$ and $^{***}p < 0.001$.

TDP-43 protein levels were assessed by Western blot. Following the mRNA expression, T43-siRNA-transfected cells showed a significant decrease (<3% of control) in TDP-43 levels compared with both MOCK and NC-siRNA-transfected cells at 72 h (Fig 3, A and B). These results indicate that T43-siRNA-transfection can achieve siRNA mediated knockdown of TDP-43.

Moreover, to evaluate the timeline of TDP-43 depletion following knockdown, we investigate the TDP-43 protein levels at 96 h and 120 h after transfection. Though the protein expression of TDP-43 gradually recovered as time goes on, protein levels of TDP-43 remained low (<11% of control) until at least 120 h after siRNA transfection

(Fig 3, A and B). Thus, T43-siRNA-mediated knockdown can keep an efficient reduction in the protein levels of TDP-43 from 72 h to 120 h.

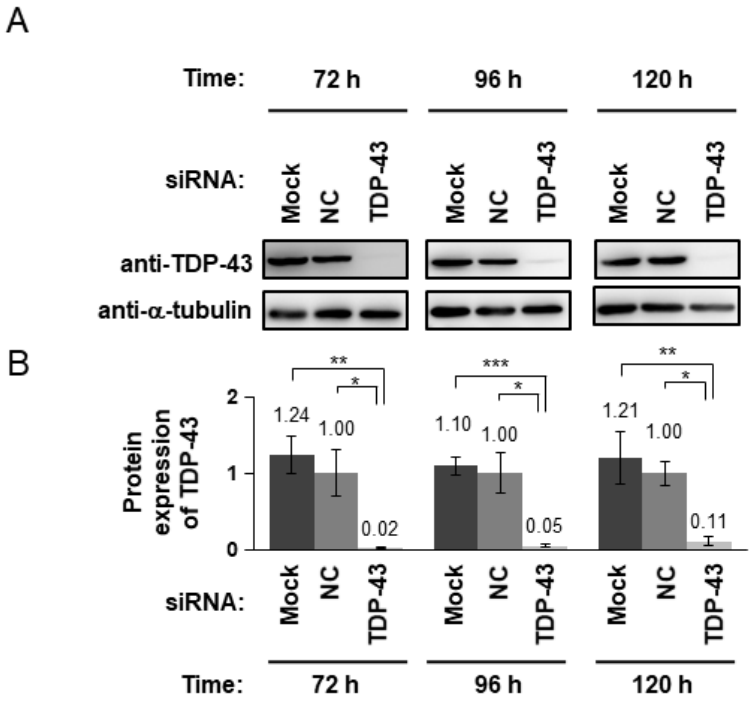

Figure 3 Time course of TDP-43 protein expression during TDP-43 knockdown. (A) Western blot analysis of endogenous protein expression of TDP-43 and α-tubulin during siRNA-mediated TDP-43 knockdown. Time after transfection of T43-siRNA, NC-siRNA (NC), or no siRNA and transfection reagents (Mock) is indicated (72, 96, and 120 h). α-tubulin was used to normalize band intensities of TDP-43. (B) Bars graphs indicate the normalized amount of endogenous TDP-43 (mean ± SEM; n = 3). Significance between indicated pairs was tested by Student's *t* test: **p* < 0.05, ***p* < 0.01, and ****p* < 0.001.

3.3. Confirmation of amplification efficiency during PCR

For precise qPCR assays, amplification efficiency during PCR (generally called as PCR efficiency) is believed to be important [34]. To investigate U6 snRNA expression during TDP-43 depletion exactly, we first checked the PCR efficiencies using the following PCR primers. Ubiquitously expressing small RNAs (18S rRNA, 7SL RNA, and snoRNA202) transcribed from housekeeping genes, were selected as internal controls for the PCR. To each targeting genes, qPCR was performed using the dilution series of PCR products as PCR template and standard curve was described. Calculated

PCR efficiency of each genes was 99.3%, U6 snRNA; 98.9%, 18S rRNA; 97.4%, 7SL RNA; and 98.7%, snoRNA202 (Fig 4A–D).

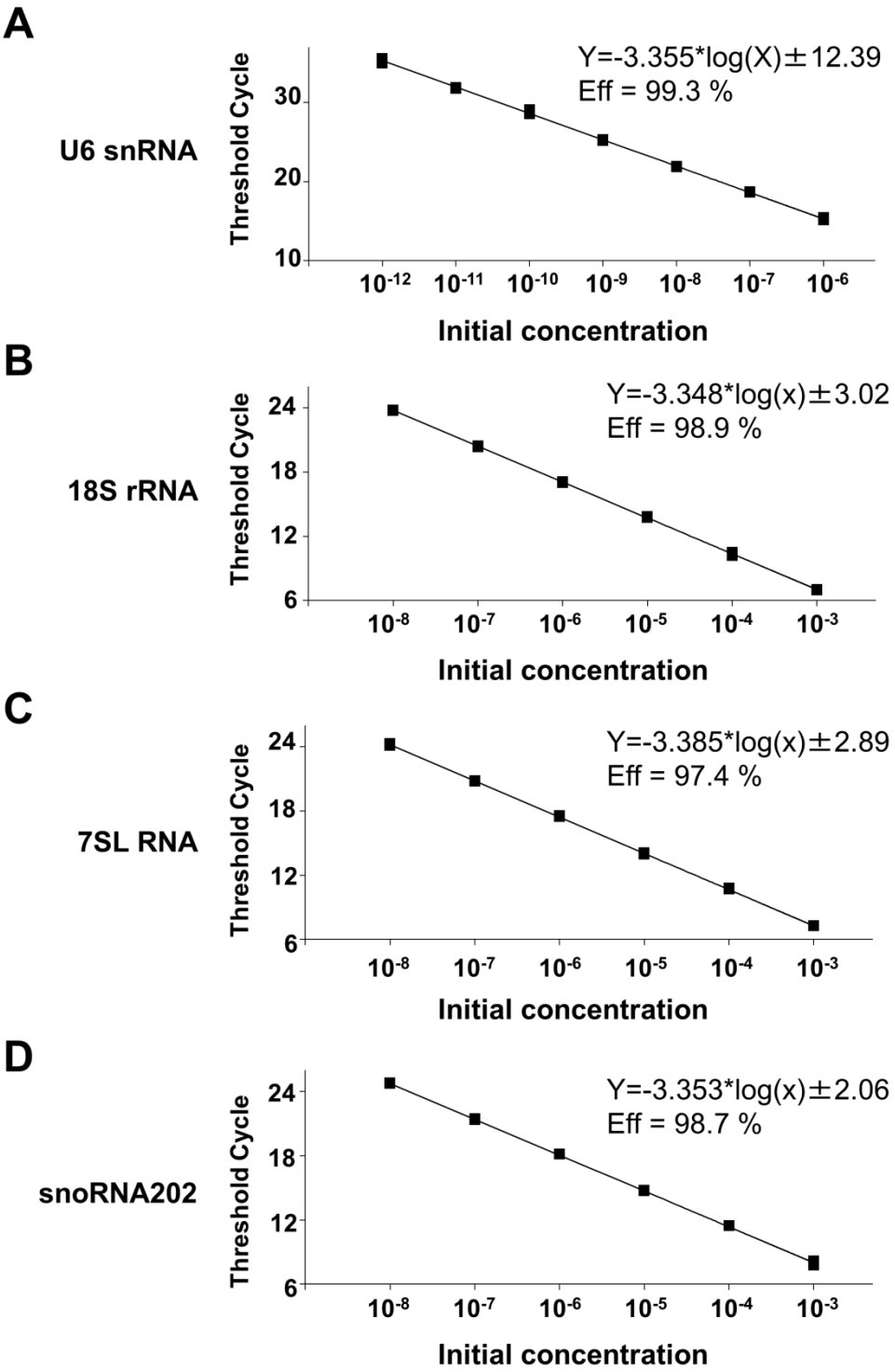

Figure 4 PCR efficiency of PCR primers. (A–D) The X axis represents the dilution ratio of the PCR template. The y axis shows the threshold cyle of each PCR primer (U6 snRNA, 18S rRNA, 7SL RNA, and snoRNA 202). The equation in the box shows the fitting result and "Eff" shows the calculated PCR efficiency.

3.4. U6 snRNA downregulation in TDP-43-knocked down cells.

Next, we checked the expression level of U6 snRNA in TDP-43-knocked down Neuro2A cells at 72 h after transfection of siRNAs by qPCR. Quantification cycle of U6 snRNA was significantly increased in T43-siRNA-transfected cells compared with NC-siRNA-transfected cells (Table 2). Using these calculated PCR efficiencies (Fig 4A–D), the relative amounts of transcripts were calculated (Fig 5). The amount of U6 snRNA in T43-siRNA-transfected cells was significantly decreased compared with that in NC-siRNA-transfected cells. The amount of 18S ribosomal RNA (18S rRNA) and 7SL RNA was not changed by TDP-43 knockdown, but that of small nucleolar RNA 202 (snoRNA202) was increased, indicating that 18S rRNA and 7SL RNA can be used as an internal control during TDP-43 depletion (Fig 5). Thus, to evaluate the amount of U6 snRNA in TDP-43-knocked down cells, we used 18S rRNA as an internal control. As a result, the expression level of U6 snRNA in TDP-43-knocked down cells was decreased to approximately 50% of that in NC-siRNA-transfected cells (Fig 6).

		U6 snRNA	18S rRNA	7SL RNA	snoRNA202
siRNA	NC	12.32± 0.32	13.23± 0.20	10.29± 0.12	16.67± 0.19
	TDP-43	13.34± 0.40	13.18± 0.09	10.28± 0.13	16.34± 0.27
p-value		0.027 *	0.299	0.680	0.105 *

Table 2 Threshold cycle of RT-qPCR results. Thresholds obtained by qPCR (Primer: U6 snRNA, 18S rRNA, 7SL RNA, and snoRNA 202) using cDNA of T43-siRNA-transfected cells or NC-siRNA-transfected cells at 72 h after siRNA transfection (mean ± SEM; n = 3). Significance was tested by Student's *t* test: *$p < 0.05$.

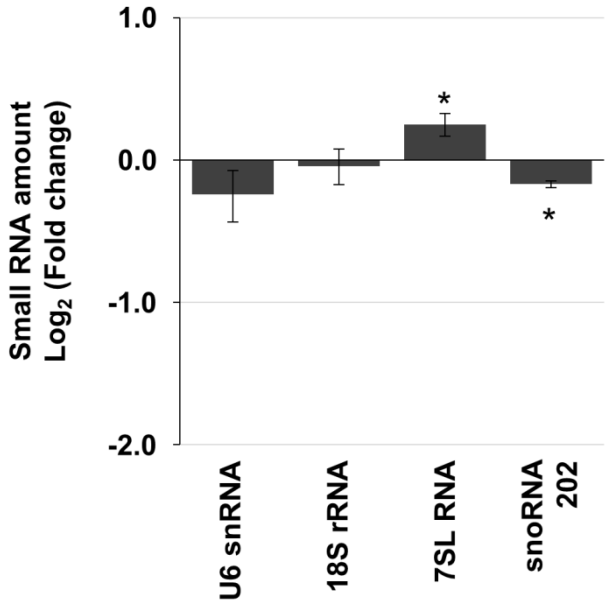

Figure 5 Fold changes in PCR-amplified amounts of small RNAs during TDP-43 knockdown. Relative PCR-amplified amounts of U6 snRNA, 18S rRNA, 7SL RNA, and snoRNA 202 in T43-siRNA-transfected cells compared with those in NC-siRNA-transfected cells at 72 h after siRNA transfection (mean ± SEM; n = 3). Significance was tested by Student's *t* test: $*p < 0.05$.

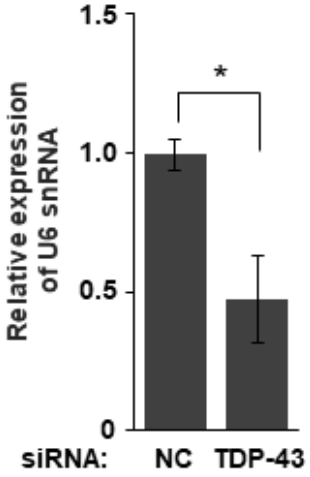

Figure 6 qPCR results of U6 snRNA in TDP-43-knocked down Neuro2A cells. Relative expression of U6 snRNA in T43-siRNA-transfected cells compared with that in NC-siRNA-transfected cells. The expression level of 18S rRNA was used as an internal control Significance was tested by Student's *t* test: $*p < 0.05$. (mean ± SEM, n = 3).

3.5. U6 snRNA selectively downregulated in TDP-43-knocked down cells.

We next elucidated the expression levels of other U snRNAs using urea-polyacrylamide gel electrophoresis (Urea-PAGE). The migration pattern of U1, U2, U4, and U6 snRNA was unequivocally assigned using their predicted molecular sizes (164, 187, 145, and 107 nucleotides, respectively). Unfortunately, U5 snRNA was not distinguished in this migration pattern (Fig 7A). The decreased amount of U6 snRNA during TDP-43 depletion was consistent with the results obtained using qPCR, whereas the amount of U1, U2, and U4 snRNA was not changed (Fig 7B). These results suggest that U6 snRNA is selectively downregulated during TDP-43 depletion in Neuro2A cells.

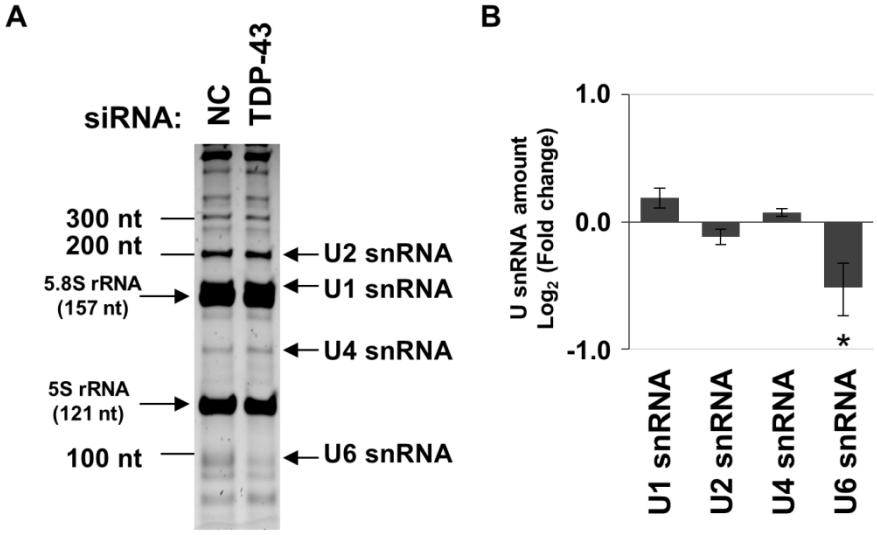

Figure 7 Urea-PAGE results of U6 snRNA in TDP-43-knocked down Neuro2A cells. (A) Gel image of Urea-PAGE. Left bar indicates molecular size in nucleotides (nt) of marker. The two dominant bands correspond to 5.8S and 5S ribosomal RNA (rRNA). (B) Relative amount of U1, U2, U4, and U6 snRNAs in T43-siRNA-transfected cells compared with that in NC-siRNA-transfected cells. Significance was tested by Student's *t* test: $*p < 0.05$ (mean ± SEM, n = 3).

3.6. TDP-43 binds to U6 snRNA.

Moreover, to investigate whether TDP-43 can associate with U6 snRNA, we quantified the amount of U6 snRNA co-immunoprecipitated with TDP-43 using qPCR. The amount of U6 snRNA did not differ between lysates of TDP-43-GFP-expressing

and GFP-expressing cells (Fig 8A; INPUT). However, the level of U6 snRNA co-precipitated with TDP43-GFP was 14.7-fold higher than that co-precipitated with GFP (Fig 8B; IP). Thus, TDP-43 may directly bind to U6 snRNA and thereby regulate its stability.

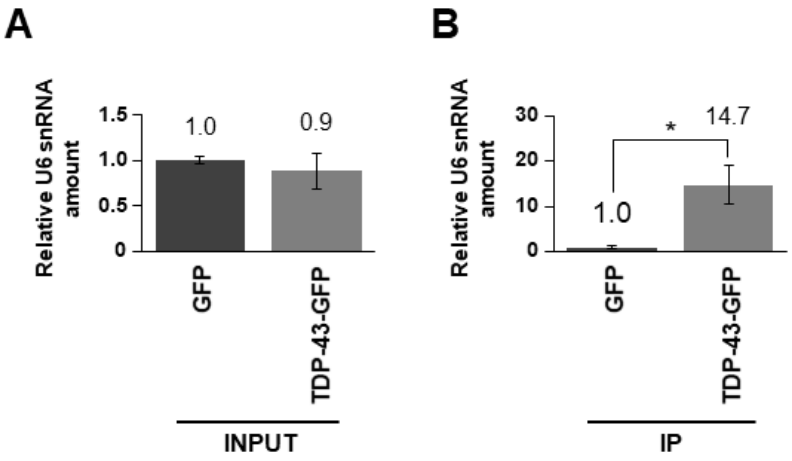

Figure 8 CLIP assay results of U6snRNA binding to TDP-43 The amount of U6 snRNA in the sample containing TDP-43-GFP was normalized against that in the sample containing GFP as a negative control in each input cell lysate (A: INPUT) or immunoprecipitated mixture (B: IP) (mean ± SEM; n = 3). Significance indicated in the graph was tested by Student's *t* test: **p* < 0.05.

3.7. Discussion

Here, we revealed that TDP-43 knockdown downregulates amount of U6 snRNA but not of U1, U2, and U4 snRNAs in mouse neuroblastoma Neuro2A cells. Since U6 snRNA expression in human neuroblastoma cells did not decreased [32,33], U6 snRNA expression was carefully examined using RT-qPCR and Urea-PAGE. Both RT-qPCR and Urea-PAGE could detect significant reduction of U6 snRNA expression indicating that reduction of U6 snRNA expression was not depended on the technical errors of RNA detection. All the quantification cycles of qPCR (Table 2) were within the quantitative range (Fig 4, A–D), supporting our data reliability.

Two possible mechanisms could explain this U6 snRNA downregulation: TDP-43 could be involved in (i) transcriptional promotion *via* RNA polymerase III and/or (ii) stability of U6 snRNA. In the first case, U6 snRNA is transcribed by RNA polymerase

III, while U1, U2, and U4 snRNAs are transcribed by RNA polymerase II [29]. However, while 7SL RNA is also transcribed by RNA polymerase III [39], our results show that 7SL RNA levels were not decreased during TDP-43 depletion (Fig 5). Therefore, transcriptional promotion *via* RNA polymerase III may not contribute to the decrease of U6 snRNA levels during TDP-43 depletion. In the second case, the U6 snRNA sequence does not contain typical UG repeats, which TDP-43 preferably recognizes; however, CLIP showed that a low amount of U6 snRNA binds to TDP-43 [24]. We confirmed that U6 snRNA co-precipitated with TDP-43-GFP (Fig 8, A and B), demonstrating that TDP-43 can associate with U6 snRNA. In addition, proteomic analysis revealed that TDP-43 interacts with SART1 and PRPF3, two components of U6 snRNA-containing complexes [40]. These findings suggest that the depletion of TDP-43 could destabilize the complex, releasing free U6 snRNA, which is likely degraded. Therefore, TDP-43 may control the stability of U6 snRNA by directly maintaining the RNA-protein complex and not *via* an intermediate process (e.g., an increased level of ribonuclease for U6 snRNA during TDP-43 depletion). However, it is unknown whether TDP-43 binds to U6 snRNA directly or *via* other proteins, and this should be clarified in a further study.

It is reported that expression level of snRNAs is unevenly altered in Spinal muscular atrophy (SMA) patients or SMA model cells [41,42]. SMA is a disease in which degeneration of motor neurons occurs same as ALS. Expression abnormality of snRNA may be predicted to be a key to neurodegeneration of motor neurons. In the chapter 3, we focused on whether the decrease in the expression level of U6 snRNA during TDP-43 depletion has physiological meaning.

Chapter 3

Rescue of U6 snRNA expression during TDP-43 depletion

1. Introduction

1.1 U6 snRNA

U6 snRNA which expression level was suppressed during TDP-43 depletion in Chapter 2 has a unique feature compared with other snRNAs. Unlike other snRNAs which are transcribed with RNA polymerase II, U6 snRNA is transcribed with RNA polymerase III [43]. Other snRNAs are delivered to the cytoplasm to become mature snRNAs, whereas U6 snRNA processing and posttranscriptional modifications are done in the nucleolus [29]. Mature U6 snRNA forms U6 snRNP complex and this complex is an essential component of splicing, responsible for recruiting U4 snRNP, U5 snRNP complex to spliceosome [29].

U6 snRNA is known as a housekeeping gene and is expressed in eukaryotic cells [29,44]. Downregulation of U6 snRNA or knockout of U6 snRNP related protein in yeast suppress proliferation efficiency [45–47]. In vitro splicing assay reveals depletion of U6 snRNP related protein has been reported to decrease splicing efficiency [48]. These facts imply that U6 snRNA plays a quite important role for cell survival and producing mature mRNA. In this chapter 3, we therefore focused on the physiological significance of U6 snRNA that is downregulated during TDP-43 depletion. Although it has been reported that the expression level of snRNAs alters under ALS and TDP-43 knockdown conditions [32,33], the physiological significance of its alteration has not been investigated. Therefore, to unveil the relationship between cell death and the alteration of U6 snRNA expression during TDP-43 depletion, we investigated whether cell death during TDP-43 depletion can be prevented by restoring the expression levels of U6 snRNA.

2. Material and methods

2.1 Plasmid DNAs

Plasmid DNAs encoding GFP (pmEGFP-N1), pmEGFP-N1 to express C-terminally GFP-tagged TDP-43 (TDP-43-GFP), plasmid DNAs encoding mCherry (pmCherry) and pmCherry to express mCherry-tagged Histone H2B (mCherry-H2B) were prepared as established previously [6].

Synthetic cDNA of TDP-43 that is not recognized by siRNA against murine TDP-43 mRNA was synthesized by Thermo Fisher Scientific (Waltham, MA). The

cDNA was subcloned into pmEGFP-N1 to express C-terminally GFP-tagged TDP-43 (T43-GFP) according to a previous study [6]. Expression of T43-GFP was observed using an laser scanning microscopy (LSM510-ConfoCor2).

Exogenous expression of U6 snRNA was driven by the human H1 promoter in the plasmid pSuperior.neo (Oligoengine, Seattle, WA). Synthetic U6 snRNA oligonucleotide was synthesized by Thermo Fisher Scientific (Table 3) and subcloned into pSuperior.neo (pU6). Empty vector (pEV) was used as a negative control.

Synthetic oligonucleotide for U6 snRNA expression plasmid	
Sense	5'-AGATCCCCGTGCTCGCTTCGGCAGCACATATACTAAAATTGGAACGATACAGAG AAGATTTAGCATGGCCCCTGCGCAAGGATGACACGCAAATTCGTGAAGCGTTCCAT ATTTTTAAGCTT-3'
Antisense	5'-AAGCTTAAAAATATGGAACGCTTCACGAATTTGCGTGTCATCCTTGCGCAGGGG CCATGCTAAATCTTCTCTGTATCGTTCCAATTTTAGTATATGTGCTGCCGAAGCGAG CACGGGGATCT-3'

Table 3 Synthetic oligonucleotides used to construct the U6 snRNA expression plasmid.

2.2 Transfection and cell preparation

The strain of the Neuro2A cells and culture conditions were described in Chapter 2. For knockdown of TDP-43 and U6 snRNA (Fig 9A), Neuro2A cells (5.5×10^5) were plated in a 10 cm cell culture dish (CORNING, Corning, NY). A sense and antisense siRNA duplex, or a non-targeting siRNA (NC-siRNA) as a negative control, were transfected using 24 μL Lipofectamine RNAiMAX transfection reagent and 160 pmol of each siRNA in Opti-MEM I medium. A synthesized sense and antisense TDP-43-targeting siRNA duplex (T43-siRNA), or a non-targeting siRNA were purchased as described in Chapter2. A sense and antisense U6 snRNA-targeting siRNA duplex (U6-siRNA; 5'-GCUUCGGCAGCACAUAUACTT-3' and 5'-GUAUAUGUGCUGCCGAAGCTT-3', respectively; synthesized by Nippon Gene) was modified from a previous study [49].

For expression of U6 snRNA in TDP-43-knocked down cells (Fig 9B), Neuro2A cells (2.8×10^5) were plated in a 10 cm culture dish. After a 20 h incubation, cells were transfected using 12.8 μL Lipofectamine 2000 transfection reagent (Thermo Fisher Scientific) and a mixture of 0.5 μg pmEGFP-N1 and either 4.5 μg pU6 or pEV. The transfection mix was incubated with the cells for 4 h. After the incubation, the medium was replaced and siRNA was transfected following the protocol described above. Cell viability assays and Western blotting were performed using 3.5 cm culture dishes and by reducing the number of cells and amounts of plasmid DNA and reagents to 1/8 scale, accordingly.

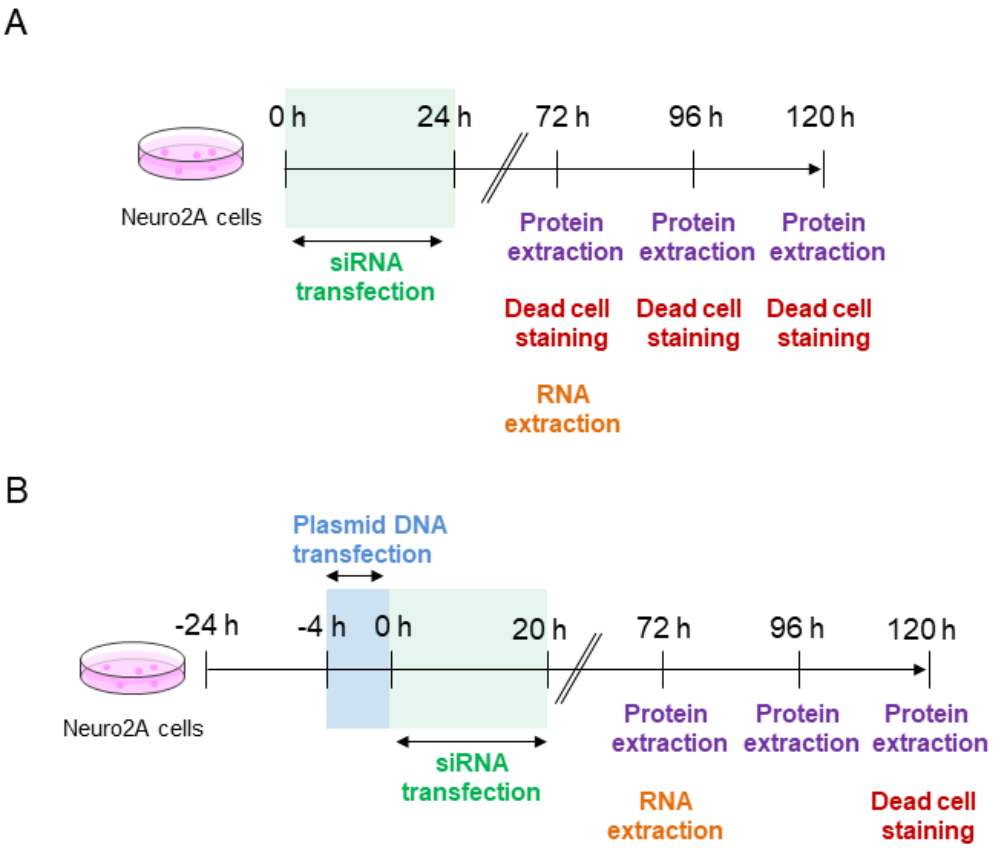

Figure 9 Schematic of the time course of transfection. (A) Transfection of T43-siRNA, total RNA extraction, protein extraction, and staining of dead cells. Green indicates the period of siRNA transfection. (B) Transfection of U6 snRNA plasmid DNA prior to transfection of T43-siRNA, total RNA extraction, protein extraction, and staining of dead cells. Blue and green indicate the period of plasmid DNA and siRNA transfection, respectively.

2.3 Western blotting

Recovery of cell lysates and Western blotting to detect the protein amount of TDP-43 and α-tubulin were performed as previously reported in Chapter 2. Proteins were detected using the anti-TDP43 (G400), α-tubulin antibody (DM1A) or anti-mCherry (#632393, Clontech, Mountain View, CA) as primary antibody and anti-rabbit IgG or anti-mouse IgG.

2.4 Cell viability assay

Dead cells were stained by 1.0 μg/mL propidium iodide (PI; Sigma-Aldrich, St. Louis, MO) and observed using an laser scanning microscopy (LSM510-ConfoCor2) and a Plan-Neofluar 10×/0.3 NA objective as reported previously [35,36].

For alternative cell viability assays based on metabolism, at 96 h after siRNA transfection, cells (0.5×10^5) in 100 μL cell culture medium were re-plated into a 96-well plate (Asahi Technoglass, Shizuoka, Japan) and cultivated for 20 h. Thereafter, 10 μL WST-1 mixture (Roche, Basel, Switzerland) was added to the cell culture medium, samples were incubated for an additional 4 h, and then the medium was collected. Absorbance at 490 and 690 nm was measured using a DU 800 spectrophotometer (Beckman Coulter, Brea, CA). Absorbance at 490 nm was subtracted from that at 690 nm.

2.5 PCR for non-coding RNAs or mRNAs

The methods of extracting total RNA and qRT-PCR for non-coding RNAs were described in Chapter 2. U6 snRNA expression was normalized using 18S rRNA expression.

To detect the splicing state of transcripts, first-strand complementary DNA synthesis was performed using a transcriptase (PrimeScript) according to the manufacturer's instructions. PCR was performed using a thermal cycler (Bioer Technology). The PCR was performed in a three-step protocol under the following conditions: initial denaturing at 98°C for 30 s, followed by PCR cycles (Dnajc5; 27 cycle, Sort1; 30 cycle, Poldip3; 28 cycle, and Madd; 28 cycle) of denaturing at 98°C for 10 s, annealing at 60°C for 30 s, and extension at 72°C for 60 s. RPS 18 was amplified as reference gene (PCR cycle; 20 cycle). PCR products were separated in 5% polyacrylamide gel and detected using LAS 4000 mini (Fujifilm, Tokyo, Japan). PCR primers are described in Table 4.

Primers for PCR		
Gene	Forward primer	Reverse primer
U6 snRNA	5'-CTCGCTTCGGCAGCACATATACT-3'	5'-ACGCTTCACGAATTTGCGTGTC-3'
18S rRNA	5'-GTAACCCGTTGAACCCCATT-3'	5'-CCATCCAATCGGTAGTAGCG-3'
RPS18	5'-GGGCGGAGATATGCTCATGTG-3'	5'-TCTGGGATCTTGTACTGTCGT-3'
Sort1	5'-CAGGAGACAAATGCCAAGGT-3'	5'-TGGCCAGGATAATAGGGACA-3'
Dnajc5	5'-CTCTATGTGGCGGAGCAGTT-3'	5'-GCTGTATGACGATCGGTGTG-3'
Poldip3/Skar	5'-AGTACAGGATGCCAGGGAGA-3'	5'-GGAGAACAGGAGCGGTGTAG-3'
Madd	5'-CTGAGCTAGGCGGTGAGTTCCCT-3'	5'-GTACTTGTGGCTCACCACTTCTTTA-3'
PPP3ca #1	5'-CTGACACTGAAGGGCCTGAC-3'	5'-GAGGTGGCATCCTCTCGTTA-3'
PPP3ca #2	5'-GAGAAGAGAGTGAGAGTGTCCTG-3'	5'-CGAGAGCCTTGTTGATGGAG-3'

Table 4 List of PCR primers.

2.6 Statistics

Student's *t* test was performed to evaluate statistical significance.

3. Results

3.1. Cell death was occurred after TDP-43 depletion.

We analyzed the timeline of cell death after TDP-43 depletion. Quantification of cell death showed that the proportion of live cells remained stable at 72 and 96 h after transfection with siRNA and significantly decreased at 120 h after siRNA transfection (Fig 10). Given that the protein level of TDP-43 was significantly decreased at 72 and 96 h after transfection (Fig 3, A and B), whereas the proportion of live cells did not significantly decrease until 120 h after siRNA treatment (Fig 10), these results indicate that there is a time lag between TDP-43 depletion and the constitution of cell death phenotype.

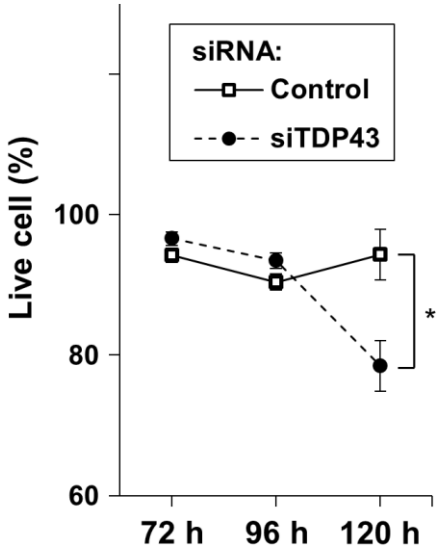

Figure 10 Time course of cell death during TDP-43 depletion. The proportion of live cells at 72, 96, and 120 h after transfection of T43-siRNA and NC-siRNA as a negative control (circle and square, respectively; mean ± SEM; n = 3). Significance between T43-siRNA- and NC-siRNA-transfected cells was tested by Student's *t* test: *$p < 0.05$.

3.2. Establishment of plasmid DNA transfection condition for siRNA-transfected cells

To rescue U6 snRNA expression in T43-siRNA-transfected Neuro2A cells, constructing a transfection system of exogenous plasmid DNA was required. Since this system is required to detect the effect of both siRNA and plasmid DNA, we first prepared a plasmid DNA coding TDP-43 tagged with GFP (T43-GFP) that is resistant to knockdown by T43-siRNA and estimated cell viability to confirm the rescue effect of TDP-43 by transfection of T43-GFP in T43-siRNA-transfected cells.

The T43-siRNA targeting region on the TDP-43 coding sequence in the plasmid DNA was replaced by the same meaning codon using synthetic DNA (T43-GFP; Fig 11A). To check the resistant ability of T43-GFP to knockdown by T43-siRNA, T43-GFP or TDP43-GFP as a control, were transfected with siRNA. Expression of T43-GFP in NC-siRNA-transfected cells was confirmed at 48 h after transfection (Fig 11B, C and D). As a result of detecting the fluorescence of GFP by microscopic observation, expression of TDP-43-GFP in T43-siRNA-transfected cells decreased compared with NC-siRNA-transfected cells, however, expression of T43-GFP did not show the remarkable changes (Fig 11B). T43-GFP was mainly localized in the nucleus as similar manner as TDP-43-GFP, indicating T43-GFP expressed TDP-43 tagged with GFP (Fig 11C). Western blot assays revealed that expression level of endogenous TDP-43 and TDP-43-GFP were suppressed by T43-siRNA, but the expression level of T43-GFP was rather increasing in T43-siRNA transfected cells (Fig 11D). These results indicate that the T43-GFP successfully acquires resistant ability to knockdown by T43-siRNA and can express TDP-43 tagged with GFP in T43-siRNA transfected cells.

A


siRNA-target-sequence
Original
CAgttagaaagaagtggaagaG
Modified
CAactggaggagcggcaggG
Amino acids
Gln Leu Glu Arg Ser Gly Arg

B

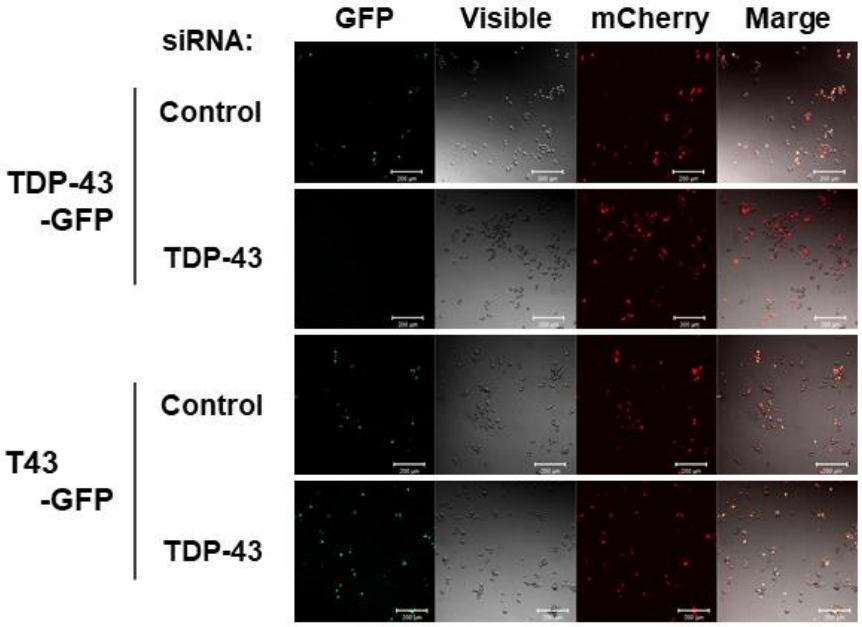
siRNA:
GFP
Visible
mCherry
Marge
TDP-43 -GFP
Control
TDP-43
T43 -GFP
Control
TDP-43

C

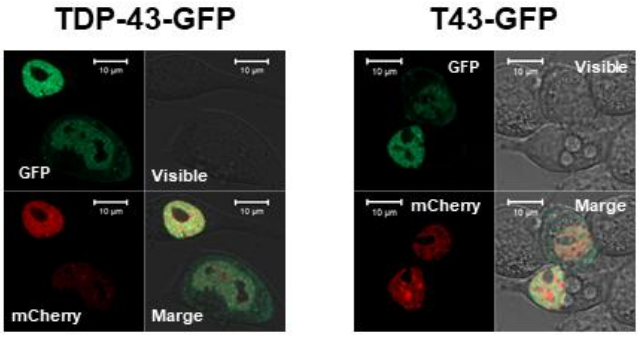
TDP-43-GFP
T43-GFP
GFP
Visible
mCherry
Marge
GFP
Visible
mCherry
Marge

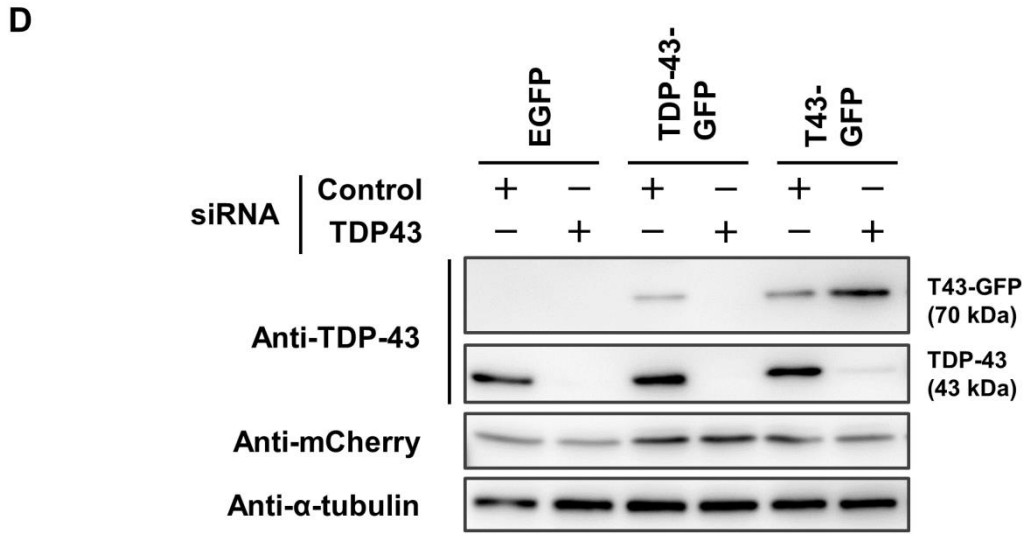

Figure 11 Expression of siRNA-resistant TDP-43-GFP (A) Original human TDP-43 cDNA sequence and modified one corresponding to siRNA-targeting region. (B) Expression of TDP-43-GFP or T43-GFP at 48 h after transfection of T43-siRNA and NC-siRNA as a negative control. mCherry was co-transfection with TDP-43-GFP or T43-GFP as a transfection marker. (C) Localization of TDP-43-GFP or T43-GFP at 48 h. mCherry-H2B was co-transfection with TDP-43-GFP or T43-GFP as a nuclear marker. (D) Western blot analysis using anti-TDP-43 antibody recognizing both endogenous and exogenous protein, anti-mCherry, or anti-α-tubulin for lysates of cells prepared in the same way in (B)

Next, we estimated that the proportion of live cells among T43-siRNA-transfected cells was restored by exogenous expression of TDP-43. T43-GFP in NC-siRNA-transfected cells did not alter the proportion of live cells (Fig 12A, lanes 1 & 2). Expression of T43-GFP in T43-siRNA-transfected cells increased the proportion of live cells (Fig 12A, lanes 3 & 4). In this case, expression of T43-GFP was confirmed at 72 h after transfection (Fig 12B). Quantification of protein levels indicated that transfection of exogenous TDP-43 resulted in a 33.2% ± 9.8% recovery of TDP-43 protein levels compared with the endogenous levels (Fig 12B, lanes 1 & 4). The 33.2% abundance of TDP-43 may be sufficient to prevent to cell death. These results indicated that the constructed transfection system of exogenous plasmid DNA in siRNA transfected cells was required to detect the cell death by TDP-43 knockdown and the rescue effect by exogenous TDP-43 expression in TDP-43 depleted cells.

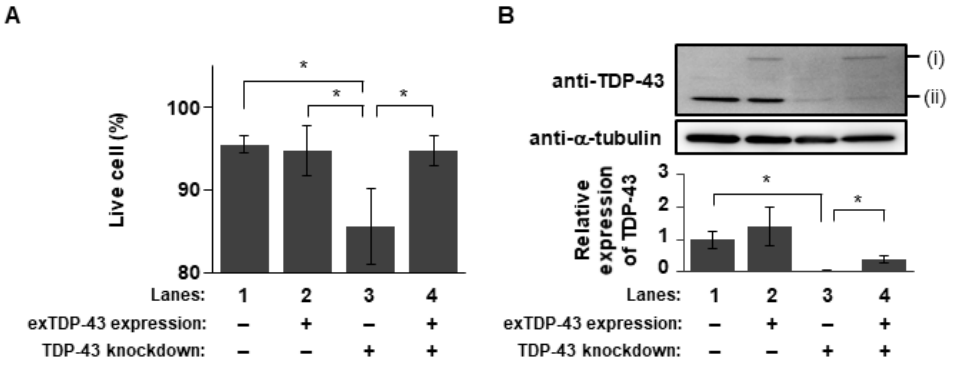

Figure 12 Amelioration of cell death by transient expression of TDP-43 in TDP-43-knocked down cells. Significance indicated in the graph was tested by Student's *t* test: **p* < 0.05 (A) The proportion of live cells at 120 h after transfection of T43-siRNA or NC-siRNA among TDP-43-expressing or control cells (mean ± SEM; n = 4). (B) Protein abundance of TDP-43 and α-tubulin during transient expression of T43-GFP for 76 h. Top: Western blotting using an anti-TDP-43 or anti-α-tubulin antibody. Bands (i) and (ii) indicate T43-GFP and endogenous TDP-43, respectively. Bottom: Quantification of relative expression of TDP-43 (mean ± SEM; n = 4).

3.3. Expression of U6 snRNA prevents cell death during TDP-43 depletion

To determine whether restoration of U6 snRNA expression rescues cell death during TDP-43 depletion, we performed the dead cell staining using PI when exogenous U6 snRNA was transiently expressed using a plasmid DNA encoding U6 snRNA (pU6) in T43-siRNA-transfected Neuro2A cells. Transfection with an empty vector (pEV) as a negative control decreased the proportion of live cells and the total number of cells during TDP-43 knockdown at 120 h (Fig 13A and B, lanes 1 & 3 to each). Interestingly, the proportion of live cells during TDP-43 knockdown was significantly restored by transfection of pU6 (Fig 13A, lanes 3 & 4), though total number of cells remained to be small (Fig 13B, lanes 3 & 4). Transfection of pU6 in NC-siRNA-transfected cells did not change the proportion of live cells (Fig 13A, lanes 1 & 2).

To confirm whether transfection of pU6 effectively increased the amount of U6 snRNA, we performed a qPCR at 76 h after transfection with pU6. The amount of U6 snRNA in NC-siRNA-transfected cells showed a slight increase by transfection with

pU6, but the difference was not significant (Fig 13C, lanes 1 & 2). A possible reason for the slight increase of U6 snRNA expression may be autoregulatory transcriptional repression during over-expression of U6 snRNA [50]. However, in the case of TDP-43 knockdown, the amount of U6 snRNA was significantly higher in pU6-transfected cells than in control pEV-transfected cells (Fig 13C, lanes 3 & 4). We therefore concluded that transient rescue of U6 snRNA expression during TDP-43 depletion can be achieved. Consequently, restoration of U6 snRNA expression efficiently slowed down the constitution of cell death phenotype during TDP-43 depletion.

While the restoration of U6 snRNA expression recovered the proportion of live cells during TDP-43 depletion, total number of cells remained to be small (Fig 13B, lanes 3 & 4). TDP-43 depletion disrupts cell proliferation through changing the expression of several proliferation factors [21,22], however, our results indicated that exogenous expression of U6 snRNA did not ameliorate these cell proliferation pathway.

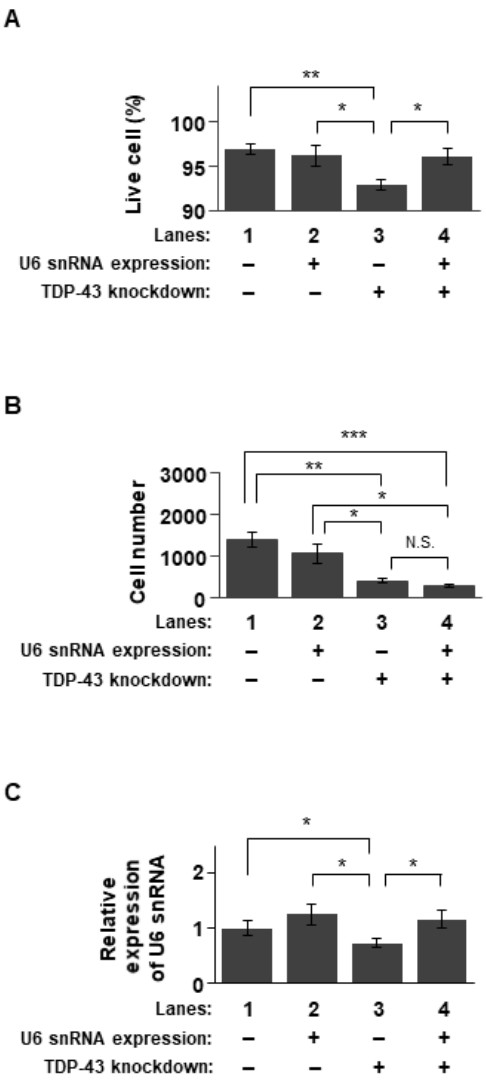

Figure 13 Amelioration of cell death by transient expression of U6 snRNA in TDP-43-knocked down cells. Significance indicated in the graph was tested by Student's *t* test: **p* < 0.05, ***p* < 0.01 and ****p* < 0.001. (A) The proportion of live cells at 120 h after transfection of T43-siRNA or NC-siRNA among U6 snRNA-expressing or non-expressing cells (mean ± SEM; n = 4). (B) The total number of cells in the view of microscopy observations at 120 h after transfection of T43-siRNA or NC-siRNA among U6 snRNA-expressing or non-expressing cells (mean ± SEM; n = 4). (C) Quantification of expression of U6 snRNA using qPCR at 72 h after transfection of U6 snRNA expression plasmid DNA or empty vector (mean ± SEM; n = 4).

Next, we checked whether exogenous expression of U6 snRNA prevents TDP-43 depletion. Exogenous expression of U6 snRNA in TDP-43-knocked down cells did not alter the amount of endogenous TDP-43 until 120 h after transfection of T43-siRNA (Fig 14A and B). Therefore, U6 snRNA may have a protective role in cell death during TDP-43 depletion.

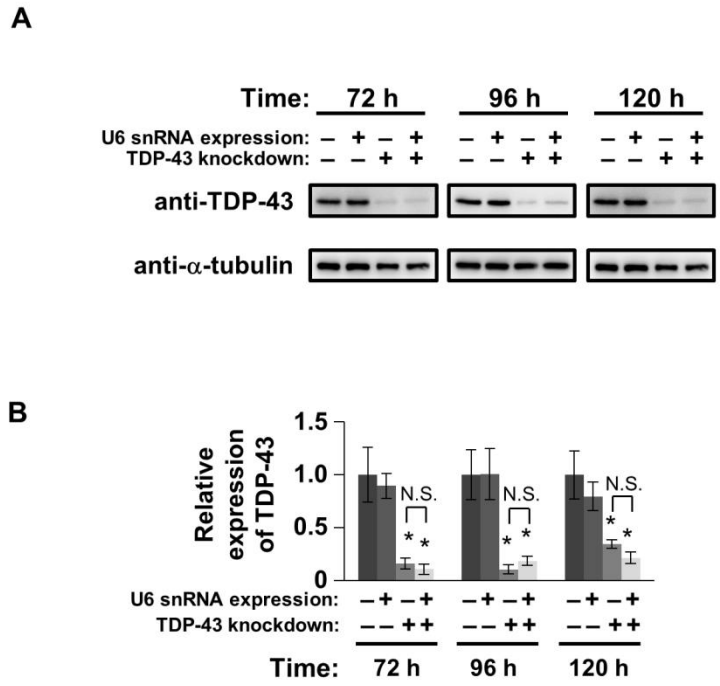

Figure 14 Time course of TDP-43 expression during transient U6 snRNA expression. (A) Western blot analysis of TDP-43 and α-tubulin in T43-siRNA- or NC-siRNA-transfected cells transiently expressing U6 snRNA. Time corresponds to the amount of time after siRNA transfection. (B) Quantification of TDP-43 expression by Western blotting using anti-TDP-43 and anti-α-tubulin antibodies (mean ± SEM; n = 3). Significance indicated in the graph was tested by Student's *t* test: **p* < 0.05. N.S. denotes no statistical significance.

3.4. Expression of U6 snRNA recovered cell survival during TDP-43 depletion.

To further confirm the rescue effect of U6 snRNA expression during TDP-43 depletion, the degree of cellular activity was examined using WST-1 that is tetrazolium salt, and can be converted to a soluble formazan dye according to cellular metabolic activity. The produced amount of formazan dye in the cell culture medium is depended on the degree of cellular activity. Therefore, by measuring the absorbance derived from formazan dye, the degree of cellular activity can be estimated [51].

First, the relationship between absorbance corresponding to the amount of formazan dye and the cell number was examined. The absorbance decreased following the reduction of the number of cells from 1.0×10^5 (A450-A690: 2.01) to 3.1×10^3 (A450-A690: 0.01), while absorbance at 1.5×10^3 (A450-A690: 0.03) showed higher value comparing to 3.1×10^3 (Fig 15). These results indicated degree of cellular activity can be estimated quantitatively within the range from 0.07 to 2.01 as the absorbance A450-A690.

Next, we investigated the degree of cellular activity when U6 snRNA expression was recovered during TDP-43 depletion. Following dead cell staining assays using PI (Fig 13A), the degree of cellular activity during TDP-43 knockdown was significantly restored by recovery of U6 snRNA expression (Fig 16, lanes 3 & 4). Thus, the fact that cell viability during TDP-43 depletion was rescued by recovery of U6 snRNA expression was confirmed in both aspects of the proportion of live cells and cellular metabolisms.

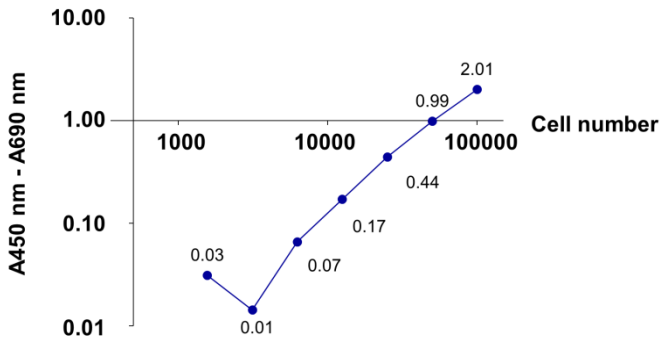

Figure 15 Calibration curve of WST-1 assay. Absorbance at 450 nm was subtracted from that at 690 nm (X axis). Total number of cells (100000, 50000, 25000, 12500, 6250, 3130 and 1560) were plated in 96 well culture dish at 24h before WST-1 addition.

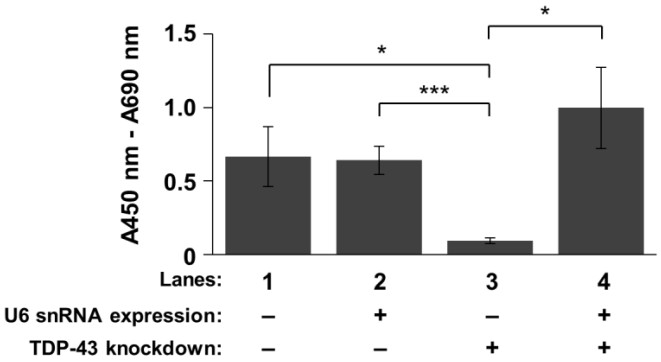

Figure 16 Quantification of the viability of TDP-43-knocked down cells transfected with U6 snRNA by the WST-1 assay. Absorbance at 450 nm was subtracted from that at 690 nm. Cells were cultured for 120 h after transfection of TDP-43-siRNA or NC-siRNA, with or without exogenous U6 snRNA expression. Significance indicated in the graph was tested by Student's *t* test: **p* < 0.05 and ****p* < 0.001 (mean ± SEM; n = 5).

3.5. Downregulation of U6 snRNA results in cell death

To investigate whether U6 snRNA is involved in cell death, U6 snRNA was knocked down using siRNA. At 72 h after transfection of U6-siRNA, U6 snRNA expression in Neuro2A cells was decreased to 72% compared with that in NC-siRNA-transfected cells (Fig 17A). The proportion of live cells was significantly decreased upon U6 snRNA knockdown (Fig 17B), indicating that downregulation of U6 snRNA increases cell death. Thus, downregulation of U6 snRNA during TDP-43 depletion may contribute to cell death. The proportion of dead cells was higher upon TDP-43 knockdown (21%, Fig 10) than upon U6 snRNA knockdown (6.5%, Fig 17B). This may be due to a difference in the degree to which U6 snRNA was downregulated (28% upon U6 snRNA knockdown and 53% upon TDP-43 knockdown).

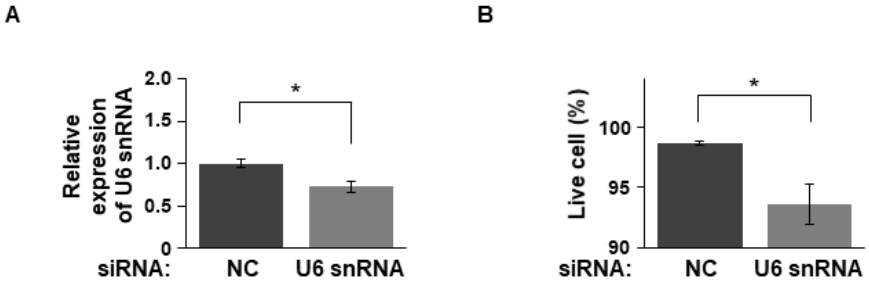

Figure 17 Viability of U6 snRNA-depleted cells. (A) Quantification of U6 snRNA expression at 72 h after transfection of U6-siRNA and NC-siRNA. The expression level of 18S rRNA was used as an internal control (mean ± SEM, n = 3). Significance was tested by Student's t test: $*p < 0.05$. (B) The proportion of live cells at 72 h after transfection of U6-siRNA and NC-siRNA (mean ± SEM; n = 3). Significance was tested by Student's t test: $*p < 0.05$.

3.6. Exogenous expression of U6 snRNA partially ameliorates mis-splicing during TDP-43 depletion

To investigate a plausible mechanism by which an increase in the U6 snRNA level ameliorates the viability of TDP-43-knocked down cells, we examined the aberrant mRNA-splicing state during TDP-43 depletion. Based on previous reports [18–20, 30], we selected four transcripts (Dnajc5, Sortilin 1 [Sort1], Poldip3, Madd, and PPP3ca) as mis-splicing targets during TDP-43 depletion. The splicing of these transcripts was

altered in TDP-43-knocked down cells (Fig 18A, lanes 1 & 3, lanes 1 & 3). We analyzed whether expression of exogenous U6 snRNA changes the amount of the spliced form of these transcripts in TDP-43-knocked down cells. The amount of the exon-excluded form of Dnajc5 and Sort1 transcripts was slightly increased by exogenous expression of U6 snRNA in TDP-43-knocked down cells (Fig 18B, lanes 3 & 4), but not in NC-siRNA-transfected cells (Fig 18B, lanes 1 & 2), whereas the splicing of Poldip3 and Madd transcripts was not changed by exogenous expression of U6 snRNA in TDP-43-knocked down cells (Fig 18B). Unfortunately, PPP3ca did expressed only exon-excluded form in Neuro2A cells (Fig 19A) and changing mRNA-splicing state could not be observed (Fig 19B). These results suggest that the splicing efficiency of Dnajc5 and Sort1 transcripts in TDP-43-knocked down cells can be partially restored by exogenous expression of U6 snRNA. Moreover, it is possible that U6 snRNA may have a protective role against the alteration of splicing efficiency of a portion of transcripts during TDP-43 depletion.

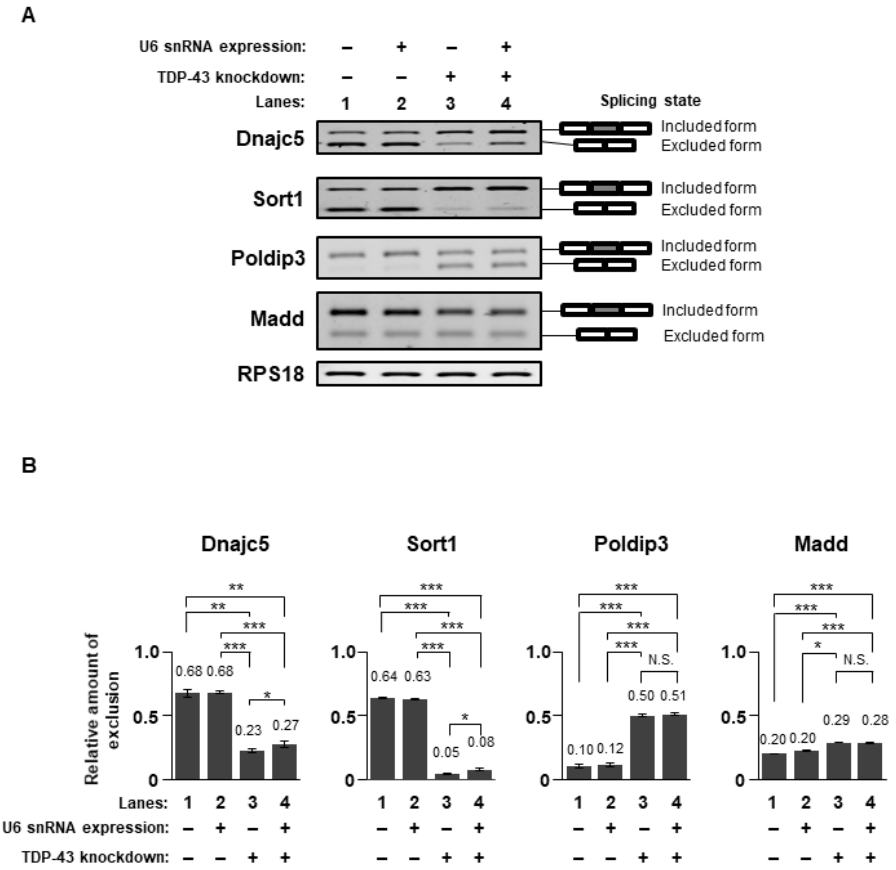

Figure 18 Change in the exon-exclusion state of transcripts during expression of U6 snRNA in TDP-43-knocked down cells. (A) Images of migrated bands of spliced forms of Dnajc5, Sort1, Poldip3 and Madd transcripts. RPS18 was used as an internal loading control. Spliced forms of transcripts were distinguished using splicing-dependent pairs of PCR primers. (B) Relative amounts of the exon-excluded forms of Dnajc5, Sort1, Poldip3 and Madd transcripts (mean ± SEM; n = 5). Significance was tested by Student's *t* test: **p* < 0.05, ***p* < 0.01, and ****p* < 0.001. Numbers in each bar show mean values.

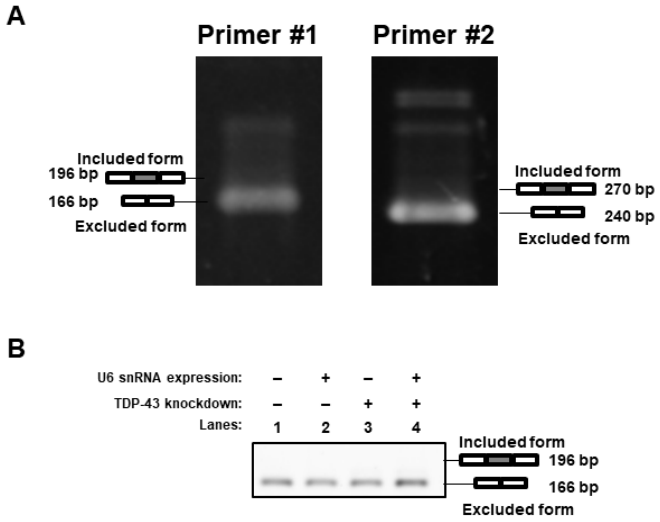

Figure 19 RT-PCR products of PPP3ca. (A) Image of migrated bands of RT-PCR products at 40 cycle using PPP3ca primers (#1 and #2). (B) Images of migrated bands at 25 cycle of spliced forms of PPP3ca transcripts during expression of U6 snRNA in TDP-43-knocked down cells.

4. Discussion

By using PI staining and WST-1 assay, we clarified that transient exogenous expression of U6 snRNA counteracted the effect of TDP-43 knockdown on cell death. Comparing the results of PI and WST-1 assay, the decrease in the proportion of live cells during TDP-43 depletion by PI staining is small, whereas cell metabolisms detected by WST-1 assay reduced dramatically.

PI staining is based on the principle that PI is capable of binding DNA in late apoptotic cells which are characterized by DNA fragmentation, and therefore, PI staining recognize late or advanced stage of cell death [52,53], indicating not all the dead cells could be detected by PI staining. On the other hand, WST-1 assay is a technic to detect the metabolic activity of cells [51], and it can be considered that the activity of the cell is sensitively reflected. Therefore, it can be reasonable that WST-1 assay exhibited greatly reduction of cell viability compared to PI staining. However, the result of PI staining based on microscopic observation is not the result of observing all the cells on the dish. Dead cells outside the view of microscopic observation may reduce the measurement accuracy. On the other hand, the accuracy of WST-1 assay could be confirmed by drawing the calibration curve (Fig15). Nevertheless, WST-1 assay needs the process of re-plating cells to culture dish for measurement at 24 h before detecting

cell metabolism, and the differences of cell condition may be expanded due to the cell damage by re-plating. Therefore, there is still room for verification regarding the accuracy of cell viability results. Importantly, recovery of cell death by exogenous expression of U6 snRNA in TDP-43 depleted cells could be detected in both PI and WST-1, and this fact is a reliable evidence of the protective role of U6 snRNA during TDP-43 depletion.

While the restoration of U6 snRNA expression recovered the proportion of live cells during TDP-43 depletion (Fig 13A), total number of cells did not recover (Fig 13B). It is reported that TDP-43 depletion disrupts cell proliferation through changing the expression of several proliferation factors [22][21]. Our results indicated that exogenous expression of U6 snRNA did not ameliorate the cell proliferation pathway.

Our results showed a time lag between the time TDP-43 depletion was confirmed (at least 72h after transfection; Fig 2 and 3) and occurrence of cell death (at 120h after transfection; Fig 10). It is only 2–3 hours that initiation of apoptosis to completion [52]. Therefore, very long time is required for promoting apoptosis by the TDP-43 depletion. It implies that TDP-43 does not directly promote apoptosis, but the time for exceeding some thresholds (e.g., accumulation of abnormal transcription products) may be necessary to promote apoptosis by TDP-43 depletion.

It is confirmed that there is also a time lag from the time the reduction of U6 snRNA in TDP-43 depleted cells (at 72h after transfection; Fig 6) to occurrence of cell death (at 120h after transfection; Fig 10). On the other hand, cell death due to U6 snRNA depletion was observed at 72 hours (Fig 17). Since siRNA can directly bind and act on RNAs [54], interference of U6 snRNA may rapidly occur after transfection of siRNA targeting U6 snRNA compared with reduction of TDP-43 protein expression after transfection of siRNA targeting TDP-43. Considering this, there may be a time lag of 72 hours before cell death was occurred by U6 snRNA depletion. Thus, the result during U6 snRNA depletion may be consistent with the time-course change observed in TDP-43 knockdown cells.

The expression of U6 snRNA in TDP-43 depleted cells slightly improved the mis-splicing efficiency of Dnajc5 and Sort1 transcripts. Dnajc5 is synaptic chaperone protein cysteine string protein and has protective role against synaptic degeneration related to Alzheimer disease [55]. Mis-splicing of Dnajc5 mRNA by TDP-43 depletion is likely to involve in neuronal cell death because exon included form of Dnajc5 mRNA generated by TDP-43 depletion is a non-sense mediated target and can reduce its expression as protein level. Sort1 is a member of a family of cellular vacuolar protein sorting 10 (VSP10)-domain receptors, and it is reported that mis-splicing of its mRNA

induces neuronal cell death through altered PGRN metabolism in humans [56]. Thus, the mis-splicing of Dnajc5 and Sort1 transcripts probably involved in cell death in TDP-43 depleted cells, and there is a possibility that recovery from mis-splicing through expression of U6 snRNA in TDP-43-knocked down cells may contribute to suppression of cell death to some extent, though its recovery ratio was very little.

Although the direct effect of U6 snRNA on the alternative splicing of transcripts in the TDP-43-knockdown condition has not been clarified yet, we expect that restoration of U6 snRNA levels during TDP-43 depletion might maintain the alternative splicing efficiency of these transcripts.

Chapter 5

General discussion and Conclusion

Although a previous study using human SH-SY5Y cells reported that the amount of U6 snRNA was not decreased by TDP-43 knockdown [32,33], we show that U6 snRNA in TDP-43-knocked down murine Neuro2A cells is downregulated in the Chapter 2. This discrepancy is likely due to differences in the species and/or cell lines, since the expression profile of U snRNAs after siRNA-mediated knockdown in survival motor neurons protein (SMN) differs between human and murine cell lines [42]. However, we clarified that expression of exogenous U6 snRNA can efficiently rescue cell death during TDP-43 depletion in the Chapter 3. These results suggest that downregulation of U6 snRNA is involved in the death of TDP-43-knocked down murine Neuro2A cells. This is the first evidence including a physiological meaning that the decreasing U6 snRNA expression during TDP-43 depletion is involved in cell death.

In addition, in Chapter 3, we investigated the change in splicing in order to investigate what mechanism is involved in cell death through reduction of U6 snRNA during TDP-43 depletion. Our results show that expression of U6 snRNA in TDP-43-knocked down cells slightly improved the mis-splicing efficiency of Dnajc5 and Sort1 transcripts. These results indicate that U6 snRNA has the protective role against mis-splicing during TDP-43 depletion, at the same time, it is probably that cell death during TDP-43 depletion is due to other effects than the mis-splicing of these genes. In this point, we assume two candidates. (i) Due to the evolution of sequencing technology, numerous number of non-conserved cryptic exons regulated by TDP-43 have been discovered [27,28]. A crucial factor of cell death during TDP-43 depletion may be included. (ii) Moreover, TDP-43 loss-of-function inhibits vesicular trafficking, including endosomal trafficking and autophagosome-lysosome fusion [20,57]. These defects may contribute to cell death by altering the trophic state. Restoration of U6 snRNA expression following TDP-43 depletion may suppress cell death by regulating the expression of genes important for trophic signaling. Thus, it is important to clarify what transcripts U6 snRNA downregulation affects during TDP-43 depletion. We hope that the genes that control cell death could likely be identified by genome-wide screening. Future studies should explore the detailed mechanisms by which downregulation of U6 snRNA expression affects alternative splicing and increases cell death upon TDP-43 depletion.

To summarize our results, U6 snRNA was identified as a new regulator against cell survival during loss-of-function of TDP-43 through maintaining the splicing or other mechanisms (Fig 20). Although our results are confined to the cellular level, a report showed a decrease in the U6 snRNA levels in spinal cord from ALS patients [32]. Therefore, we expect that downregulation of U6 snRNA might be involved in

loss-of-function of TDP-43 in ALS pathophysiology and correction of U6 snRNA expression might slow down neuronal cell death during TDP-43 loss-of-function in ALS patients. Thus, investigations of an endogenous mechanism and/or drug to maintain the expression levels of U6 snRNA during loss-of-function of TDP-43 would lead to the elucidation of ALS pathophysiology.

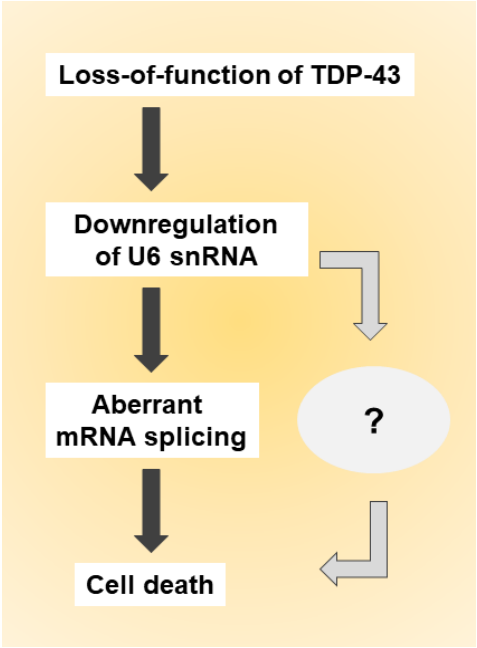

Figure 20 The proposed model leading to cell death during loss-of-function of TDP-43

Acknowledgement

I would like to appreciate my supervisor Prof. Masataka Kinjo for giving the theme "Study on mechanism of neuronal cell death in amyotrophic lateral sclerosis using U6 snRNA expression analysis". In promoting of this thesis, he gave me polite and enthusiastic guidance. I express my gratitude here.

In promoting this research, I would like to thank Dr. Akira Kitamura who received me not only the guidance but also many knowledge and suggestions through daily discussion. Without his advices, this research could not proceed. I would like to express my gratitude here.

I would like to thank Dr. Mikuni who gave various experimental techniques in this research. When my research is in impasse, his advice opened up ahead.

Also, I thank the all the Kinjo laboratory members and class mates in Biological Sciences (Macromolecular Functions) and Graduate School of Life Science of Hokkaido university who received much knowledge and suggestions through daily discussions and life.

Finally, I would like to express my gratitude to my parents who gave me the opportunity to learn at Hokkaido University and my aunt, Kazuyo Sato, for financially supporting me during my studies.

Reference

1. Esteller, M. Non-coding RNAs in human disease. *Nat. Rev. Genet.* **12,** 861–874 (2011).
2. Belzil, V. V., Gendron, T. F. & Petrucelli, L. RNA-mediated toxicity in neurodegenerative disease. *Mol. Cell. Neurosci.* **56,** 406–419 (2013).
3. Anthony, K. & Gallo, J. M. Aberrant RNA processing events in neurological disorders. *Brain Res.* **1338,** 67–77 (2010).
4. Mills, J. D. & Janitz, M. Alternative splicing of mRNA in the molecular pathology of neurodegenerative diseases. *Neurobiol. Aging* **33,** 1012.e11-1012.e24 (2012).
5. Scotti, M. M. & Swanson, M. S. RNA mis-splicing in disease. *Nat. Rev. Genet.* **17,** 19–32 (2015).
6. Donnelly, C. J., Grima, J. C. & Sattler, R. Aberrant RNA homeostasis in amyotrophic lateral sclerosis : potential for new therapeutic targets? *Neurodegener. Dis. Manag.* **4,** 417–437 (2014).
7. Robberecht, W. & Philips, T. The changing scene of amyotrophic lateral sclerosis. *Nat. Rev. Neurosci.* **14,** 248–264 (2013).
8. Aulas, A. & Vande Velde, C. Alterations in stress granule dynamics driven by TDP-43 and FUS: a link to pathological inclusions in ALS? *Front. Cell. Neurosci.* **9,** 1–13 (2015).
9. Mackenzie, I. R. A., Rademakers, R. & Neumann, M. TDP-43 and FUS in amyotrophic lateral sclerosis and frontotemporal dementia. *Lancet Neurol.* **9,** 995–1007 (2010).
10. Lagier-Tourenne, C., Polymenidou, M. & Cleveland, D. W. TDP-43 and FUS/TLS: Emerging roles in RNA processing and neurodegeneration. *Hum. Mol. Genet.* **19,** 46–64 (2010).
11. Neumann, M., Sampathu, D. M., Kwong, L. K., *et al.* Ubiquitinated TDP-43 in frontotemporal lobar degeneration and amyotrophic lateral sclerosis. *Science* **314,** 130–133 (2006).
12. Wils, H., Kleinberger, G., Janssens, J., *et al.* TDP-43 transgenic mice develop spastic paralysis and neuronal inclusions characteristic of ALS and frontotemporal lobar degeneration. *Proc. Natl. Acad. Sci. U. S. A.* **107,** 3858–63 (2010).
13. Zhang, Y.-J., Xu, Y.-F., Cook, C., *et al.* Aberrant cleavage of TDP-43 enhances aggregation and cellular toxicity. *Proc. Natl. Acad. Sci. U. S. A.* **106,** 7607–7612

(2009).
14. Liu, Y., Duan, W., Guo, Y., *et al.* A new cellular model of pathological TDP-43: The neurotoxicity of stably expressed CTF25 of TDP-43 depends on the proteasome. *Neuroscience* **281,** 88–98 (2014).
15. Iguchi, Y., Katsuno, M., Niwa, J. -i., *et al.* Loss of TDP-43 causes age-dependent progressive motor neuron degeneration. *Brain* **136,** 1371–1382 (2013).
16. Wu, L.-S. S., Cheng, W.-C. C., Hou, S.-C. C., *et al.* TDP-43, a neuro-pathosignature factor, is essential for early mouse embryogenesis. *Genesis* **48,** 56–62 (2016).
17. Pesiridis, G. S., Tripathy, K., Tanik, S., *et al.* A 'two-hit' hypothesis for inclusion formation by carboxyl-terminal fragments of TDP-43 protein linked to RNA depletion and impaired microtubule-dependent transport. *J. Biol. Chem.* **286,** 18845–18855 (2011).
18. Kraemer, B. C., Schuck, T., Wheeler, J. M., *et al.* Loss of Murine TDP-43 disrupts motor function and plays an essential role in embryogenesis. *Acta Neuropathol.* **119,** 409–419 (2010).
19. Iguchi, Y., Katsuno, M., Niwa, J., *et al.* TDP-43 Depletion Induces Neuronal Cell Damage through Dysregulation of Rho Family GTPases. *J. Biol. Chem.* **284,** 22059–22066 (2009).
20. Xia, Q., Wang, H., Hao, Z., *et al.* TDP-43 loss of function increases TFEB activity and blocks autophagosome–lysosome fusion. *EMBO J.* **35,** 121–142 (2016).
21. Chiang, P., Ling, J., Ha, Y., *et al.* Deletion of TDP-43 down-regulates Tbc1d1, a gene linked to obesity, and alters body fat metabolism. *Proc. Natl. Acad. Sci. U. S. A.* **107,** 16320–16324 (2010).
22. Ayala, Y. M., Misteli, T. & Baralle, F. E. TDP-43 regulates retinoblastoma protein phosphorylation through the repression of cyclin-dependent kinase 6 expression. *Proc. Natl. Acad. Sci. U. S. A.* **105,** 3785–3789 (2008).
23. Polymenidou, M., Lagier-tourenne, C., Hutt, K. R., *et al.* Long pre-mRNA depletion and RNA missplicing contribute to neuronal vulnerability from loss of TDP-43. *Nat. Neurosci.* **14,** 459–468 (2011).
24. Lagier-Tourenne, C., Polymenidou, M., Hutt, K. R., *et al.* Divergent roles of ALS-linked proteins FUS/TLS and TDP-43 intersect in processing long pre-mRNAs. *Nat. Neurosci.* **15,** 1488–1497 (2012).
25. Arnold, E. S., Ling, S.-C., Huelga, S. C., *et al.* ALS-linked TDP-43 mutations produce aberrant RNA splicing and adult-onset motor neuron disease without

aggregation or loss of nuclear TDP-43. *Proc. Natl. Acad. Sci. U. S. A.* **110,** 736–745 (2013).

26. Tollervey, J. R., Curk, T., Rogelj, B., *et al.* Characterising the RNA targets and position-dependent splicing regulation by TDP-43; implications for neurodegenerative diseases. *Nat. Neurosci.* **14,** 452–458 (2011).
27. Ling, J. P., Pletnikova, O., Troncoso, J. C. & Wong, P. C. TDP-43 repression of nonconserved cryptic exons is compromised in ALS-FTD. *Science.* **349,** 650–655 (2015).
28. Tan, Q., Hari Krishna Yalamanchili, Park, J., *et al.* Extensive cryptic splicing upon loss of RBM17 and TDP43 in neurodegeneration models. *Hum. Mol. Genet.* **25,** 1–38 (2016).
29. Mroczek, S. & Dziembowski, A. U6 RNA biogenesis and disease association. *Wiley Interdiscip. Rev. RNA* **4,** 581–592 (2013).
30. Matter, N. & K??nig, H. Targeted 'knockdown' of spliceosome function in mammalian cells. *Nucleic Acids Res.* **33,** 1–5 (2005).
31. Okeefe, R. T., Mayeda, A., Sadowski, C. L., *et al.* Disruption of pre-messenger RNA splicing in vivo results in reorganization of splicing factors. *J Cell Biol* **124,** 249–260 (1994).
32. Ishihara, T., Ariizumi, Y., Shiga, A., *et al.* Decreased number of gemini of coiled bodies and U12 snRNA level in amyotrophic lateral sclerosis. *Hum. Mol. Genet.* **22,** 4136–4147 (2013).
33. Tsuiji, H., Iguchi, Y., Furuya, A., *et al.* Spliceosome integrity is defective in the motor neuron diseases ALS and SMA. *EMBO Mol. Med.* **5,** 221–234 (2013).
34. Bustin, S. A., Benes, V., Garson, J. A., *et al.* The MIQE Guidelines: Minimum Information for Publication of Quantitative Real-Time PCR Experiments. *Clin. Chem.* **55,** 611–622 (2009).
35. Kitamura, A., Nakayama, Y., Shibasaki, A., *et al.* Interaction of RNA with a C-terminal fragment of the amyotrophic lateral sclerosis- associated TDP43 reduces cytotoxicity. *Sci. Rep.* **6,** 19230–19230 (2016).
36. Kitamura, A., Kubota, H., Pack, C.-G., *et al.* Cytosolic chaperonin prevents polyglutamine toxicity with altering the aggregation state. *Nat. Cell Biol.* **8,** 1163–1170 (2006).
37. Pfaffl, M. W. A new mathematical model for relative quantification in real-time RT-PCR. *Nucleic Acids Res.* **29,** 45e–45 (2001).
38. Vogt, M. & Taylor, V. Cross-linked RNA Immunoprecipitation. *Bio-Protocol* **3,** e398 (2013).

39. Dieci, G., Fiorino, G., Castelnuovo, M., *et al.* The expanding RNA polymerase III transcriptome. *Trends Genet.* **23,** 614–622 (2007).
40. Freibaum, B. D., Chitta, R., High, A. a & Taylor, J. P. Global analysis of TDP-43 interacting proteins reveals strong association with RNA splicing and translation machinery. *J Proteome Res.* **9,** 1104–1120 (2011).
41. Boulisfane, N., Choleza, M., Rage, F., *et al.* Impaired minor tri-snRNP assembly generates differential splicing defects of U12-type introns in lymphoblasts derived from a type I SMA patient. *Hum. Mol. Genet.* **20,** 641–648 (2011).
42. Zhang, Z., Lotti, F., Dittmar, K., *et al.* SMN Deficiency Causes Tissue-Specific Perturbations in the Repertoire of snRNAs and Widespread Defects in Splicing. *Cell* **133,** 585–600 (2008).
43. Kunkel, G. R., Maser, R. L., Calvet, J. P. & Pederson, T. U6 small nuclear RNA is transcribed by RNA polymerase III. *Proc. Natl. Acad. Sci. U. S. A.* **83,** 8575–9 (1986).
44. van Wijngaarden, P., Brereton, H. M., Coster, D. J. & Williams, K. A. Stability of housekeeping gene expression in the rat retina during exposure to cyclic hyperoxia. *Mol. Vis.* **13,** 1508–1515 (2007).
45. Shchepachev, V., Wischnewski, H., Missiaglia, E., *et al.* Mpn1, Mutated in Poikiloderma with Neutropenia Protein 1, Is a Conserved 3'-to-5' RNA Exonuclease Processing U6 Small Nuclear RNA. *Cell Rep.* **2,** 855–865 (2012).
46. Mayes, A. E., Verdone, L., Legrain, P. & Beggs, J. D. Characterization of Sm-like proteins in yeast and their association with U6 snRNA. *EMBO J.* **18,** 4321–4331 (1999).
47. Luhtala, N. & Parker, R. LSM1 over-expression in Saccharomyces cerevisiae depletes U6 snRNA levels. *Nucleic Acids Res.* **37,** 5529–5536 (2009).
48. Makarova, O. V., Makarov, E. M. & Lührmann, R. The 65 and 110 kDA SR-related proteins of the U4/U6·U5 tri-snRNP are essential for the assembly of mature spliceosomes. *EMBO J.* **20,** 2553–2563 (2001).
49. Robb, G. B., Brown, K. M., Khurana, J. & Rana, T. M. Specific and potent RNAi in the nucleus of human cells. *Nat. Struct. Mol. Biol.* **12,** 133–137 (2005).
50. Noonberg, S. B., Scott, G. K. & Benz, C. C. Evidence of post-transcriptional regulation of U6 small nuclear RNA. *J. Biol. Chem.* **271,** 10477–10481 (1996).
51. Ishiyama, M., Shiga, M., Sasamoto, K., *et al.* A New Sulfonated Tetrazolium Salt That Produces a Highly Water-Soluble Formazan Dye. *Chem. Pharm. Bull.* **41,** 1118–1122 (1993).
52. Riccardi, C. & Nicoletti, I. Analysis of apoptosis by propidium iodide staining

and flow cytometry. *Nat. Protoc.* **1,** 1458–1461 (2006).

53. Elstein, K. H. & Zucker, R. M. Comparison of Cellular and Nuclear Flow Cytometric Techniques for Discriminating Apoptotic Subpopulations. *Exp. Cell Res.* **211,** 322–331 (1994).
54. Carthew, R. W. & Sontheimer, E. J. Origins and Mechanisms of miRNAs and siRNAs. *Cell* **136,** 642–655 (2009).
55. Tiwari, S. S., D Orange, M., Troakes, C., *et al.* Evidence that the presynaptic vesicle protein CSPalpha is a key player in synaptic degeneration and protection in Alzheimer's disease. *Mol. Brain* **8,** 6 (2015).
56. Prudencio, M., Jansen-West, K. R., Lee, W. C., *et al.* Misregulation of human sortilin splicing leads to the generation of a nonfunctional progranulin receptor. *Proc. Natl. Acad. Sci. U. S. A.* **109,** 21510–5 (2012).
57. Schwenk, B. M., Hartmann, H., Serdaroglu, A., *et al.* TDP-43 loss of function inhibits endosomal trafficking and alters trophic signaling in neurons. *EMBO J.* **35,** 2350–2370 (2016).